

# Optimized puncturing distributions for irregular non-binary LDPC codes

Matteo Gorgoglione\*, Valentin Savin\*, David Declercq<sup>†</sup>

\*CEA-LETI, MINATEC, Grenoble, France, {valentin.savin, matteo.gorgoglione}@cea.fr

<sup>†</sup>ETIS ENSEA/univ. Cergy-Pontoise/CNRS, Cergy-Pontoise, France, declercq@ensea.fr

**Abstract**— In this paper we design non-uniform bit-wise puncturing distributions for irregular non-binary LDPC (NB-LDPC) codes. The puncturing distributions are optimized by minimizing the decoding threshold of the punctured LDPC code, the threshold being computed with a Monte-Carlo implementation of Density Evolution. First, we show that Density Evolution computed with Monte-Carlo simulations provides accurate (very close) and precise (small variance) estimates of NB-LDPC code ensemble thresholds. Based on the proposed method, we analyze several puncturing distributions for regular and semi-regular codes, obtained either by clustering punctured bits, or spreading them over the symbol-nodes of the Tanner graph. Finally, optimized puncturing distributions for non-binary LDPC codes with small maximum degree are presented, which exhibit a gap between 0.2 and 0.5 dB to the channel capacity, for punctured rates varying from 0.5 to 0.9.

## I. INTRODUCTION

In the modern approach of error correcting codes, binary Low-Density Parity-Check (LDPC) codes are playing a very important role due to their low decoding complexity and to the fact that they can be optimized for a broad class of channels, with asymptotic performance approaching the theoretical Shannon limit [1]. On the other hand, LDPC codes over non-binary alphabets exhibit better performance for short to medium code lengths [2], without sacrificing the almost optimal asymptotic performance. The performance gain at short length comes at an additional cost in the decoding complexity. However, this additional cost can be reduced by using sub-optimal low complexity algorithms, as proposed e.g. in [3], [4]. When coded bits are transmitted over time-varying channels, as for wireless communication systems, the rate of the forward error correction code has to be adapted to the quality of the channel, so as to achieve both high throughput and reliability. Rate adaptation requires codes of different rates, which can be efficiently obtained by using one low rate mother code and puncture it to get higher rates. The advantage of puncturing is that the same decoder can be used regardless the puncturing pattern: according to the channel conditions, the transmission system adapts by just changing the puncturing pattern at the transmitter, and the depuncturing pattern at the receiver.

In this work we explore the rate-adaptability behavior of non-binary LDPC codes. In the binary case, Ha et al. [5] showed that puncturing patterns can be optimized so that rate-compatible puncturing results in a small loss of the

asymptotical performance (threshold). For non-binary codes, Klinc et al. [6] proposed a design of puncturing patterns based on symbol recovery levels, similar to the design proposed in the binary case in [7]. Given a target punctured rate, the algorithm proposed in [7] computes a puncturing pattern that minimizes the number of recovery steps for the punctured bits. This approach is thought for finite length puncturing design, but does not give insights regarding the optimization of the puncturing distribution, for LDPC code ensembles.

In the binary case, the puncturing distribution is defined by fractions  $\{f_d\}_d$  of punctured bit-nodes of degree  $d$ . For non-binary codes, the puncturing distribution can be defined in terms of fractions  $\{f_{d,k}\}_{d,k}$  of degree- $d$  symbol-nodes with exactly  $k$  punctured bits per symbol. Note that addressing the problem of the optimization of puncturing distributions is compliant with the finite length approach of [6], and from an optimized puncturing distribution, one can advantageously use the algorithm proposed in [6] in order to construct the actual puncturing pattern <sup>1</sup>.

Although the study of non-binary LDPC codes is mainly motivated by their performance at short to medium lengths, their asymptotic analysis proves also to be very useful. In particular, it allows the understanding of topology independent phenomena or, stated differently, it allows distinguishing between events due to code family parameters, and those due to a particular code realization. The asymptotical performance of an ensemble of codes is referred to as *threshold*, and corresponds to the worst channel condition that allows transmission with an arbitrary small error probability when the code length tends to infinity. It can be determined by the concept of density evolution [8]. Unfortunately, for the non-binary case, exact density evolution is only manageable for the Erasure Channel [9], [10]. In the case of more general memoryless channels, like the binary-input AWGN channel, density evolution must be approximated using numerical techniques, or approached by modeling the density of the messages, e.g. with a Gaussian approximation [11].

In this work we show that density evolution of non-binary LDPC codes can be tightly approximated by using fast Monte-Carlo approximation of the density of the messages exchanged

<sup>1</sup>As a parallel, consider the construction of bipartite Tanner graphs: for given node-degree distributions, we can advantageously use the Progressive Edge Growth (PEG) algorithm, so as to maximize the girth of the constructed graph; however, if the PEG algorithm is not constrained with a given degree distribution, the algorithm will tend to construct a regular graph, which does not provide the best performance

during the iterative decoding of an infinite code. This method allows for obtaining very close estimates of thresholds of non-binary ensembles, making possible the optimization of non-binary codes for a wide range of applications and channel models. In particular, it can be successfully applied for optimizing puncturing distributions for rate-compatible non-binary LDPC codes. We used genetic optimization methods for searching good puncturing distributions for non-binary LDPC codes over  $\mathbb{F}_{16}$ , with maximum symbol-node degree equal to 10. Optimized distributions exhibit a gap to capacity between 0.2 and 0.5dB, for punctured rates varying from 0.5 to 0.9.

The rest of the paper is organized as follows. In Section II we introduce the notations and review some basics on non binary LDPC codes. Section III presents the proposed method for approximating the density evolution of non-binary LDPC codes. Puncturing distributions are introduced in Section IV, and clustering vs. spreading distributions are analyzed for regular and semi-regular codes in Section V. The optimization of puncturing distributions for irregular codes is addressed in Section VI. Finally, Section VII concludes the paper.

## II. NON BINARY LDPC CODES

We consider non-binary codes defined over  $\mathbb{F}_q$ , the finite field with  $q$  elements, where  $q = 2^p$  is a power of 2 (the last condition is only assumed for practical reasons). We fix once for all a vector space isomorphism:

$$\mathbb{F}_q \xrightarrow{\sim} \mathbb{F}_2^p, \quad (1)$$

and we say that  $(x_0, \dots, x_{p-1}) \in \mathbb{F}_2^p$  is the *binary image* of the symbol  $X \in \mathbb{F}_q$  if they correspond to each other by the above isomorphism. An LDPC code over  $\mathbb{F}_q$  is defined as the kernel of a sparse parity-check matrix  $H \in \mathbf{M}_{M,N}(\mathbb{F}_q)$ . The matrix  $H$  can be represented by a bipartite graph comprising  $M$  constraint-nodes and  $N$  symbol-nodes, associated respectively with its  $M$  rows and its  $N$  columns. A constraint-node and a symbol-node are connected by an edge if the corresponding entry of  $H$  is non-zero. Each edge of the graph is further labeled by the corresponding non-zero entry. Thus, symbol-nodes represent coded symbols, while constraint-nodes together with edge labels correspond to linear constraints on these symbols. The number of edges incident to a node is referred to as node degree. Interconnections between nodes are usually expressed by the edge-perspective degree distribution polynomials  $\lambda(x) = \sum_d \lambda_d x^{d-1}$  and  $\rho(x) = \sum_d \rho_d x^{d-1}$ , where  $\lambda_d$  and  $\rho_d$  represent the fraction of edges connected respectively to symbol and constraint-nodes of degree  $d$ . We denote by  $r$  the design coding rate, which is given by  $r = 1 - \frac{\int_0^1 \rho(x) dx}{\int_0^1 \lambda(x) dx}$ . It is well known that the asymptotic performance of binary LDPC codes depends only on these degree distribution polynomials [8]. For non-binary codes, the performance can be slightly improved by choosing optimized distributions of edge labels [10]. However, in general this improvement seems to be minimal; therefore, in the next section we will consider ensembles  $\mathcal{E}_q(\lambda, \rho)$ , of non-binary LDPC codes over  $\mathbb{F}_q$ , with edge-perspective

degree distribution polynomials  $\lambda$  and  $\rho$ , and with edge labels uniformly distributed over  $\mathbb{F}_q^*$ .

## III. ASYMPTOTIC PERFORMANCE OF NON-BINARY LDPC CODES

Consider some channel model depending on a parameter  $s$ , such that the channel conditions worsen when  $s$  increases (for instance, the noise variance for the AWGN channel, or the erasure probability for the BEC channel). The *threshold* of the ensemble  $\mathcal{E}_q(\lambda, \rho)$  is defined as the supremum value of  $s$  (worst channel condition) that allows transmission with an arbitrary small error probability, assuming that the transmitted data is encoded with an arbitrary-length code of  $\mathcal{E}_q(\lambda, \rho)$ . For symmetric channels, we can assume that the all-zero codeword is transmitted, and the threshold can be approximated by simulating the density evolution of messages exchanged within the iterative decoding of an “infinite” code from the ensemble [12]. For doing so, we have to ensure that exchanged messages remain uncorrelated for a large number of iterations. Since the density evolution is observed on a finite number of exchanged messages, we proceed as described below in order to decorrelate them. Consider that we have to compute an outgoing message (either from a symbol, or a constraint-node). First, we sample the node degree  $d$  according to the corresponding degree distribution (either  $\lambda$ , or  $\rho$ ), and we randomly choose  $d - 1$  messages from those produced at the previous half iteration. These messages are considered as being received by the node on the  $d - 1$  incoming edges, and  $d - 1$  edge labels are also uniformly sampled from  $\mathbb{F}_q^*$ . Besides, in order to compute outgoing messages from symbol-nodes, we also need the knowledge the a priori information corresponding to the channel output. In this case, for each new outgoing symbol-node message, the channel output is also resampled according to the channel model. The outgoing message is then computed according to the Sum-Product decoding rules [13]. This is illustrated at Figure 1 for  $\lambda(x) = \frac{1}{3}x + \frac{2}{3}x^3$  and  $\rho(x) = x^5$  (designed code rate  $r = 1/2$ ), where outgoing symbol and constraint-node messages are respectively denoted by  $\alpha_i$  and  $\beta_j$ , edge labels are denoted by  $h_{i,j}$ , and the a priori information corresponding to the channel output by  $\gamma_i$ . We also remark that exchanged messages are better decorrelated for higher order finite fields, due to the edge-labels resampling.

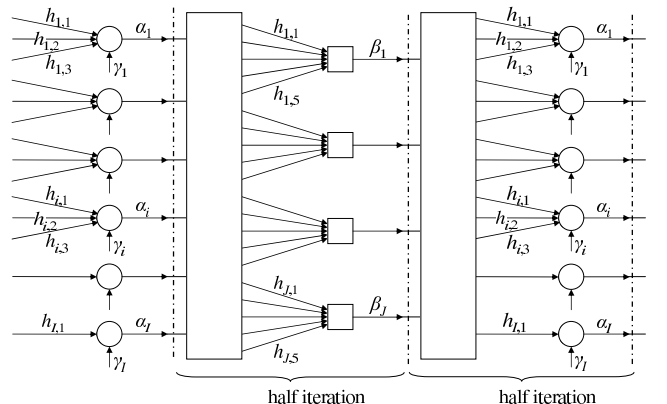


Fig. 1. Density evolution approximation by Monte-Carlo simulation

TABLE I  
THRESHOLDS FOR BINARY IRREGULAR LDPC CODES

$d_{\max}$	Exact-DE		GA-DE		MC-DE		$\sigma_{\text{dev}}^* \times 10^3$
	$\sigma^*$	$E_b/N_0^*$	$\sigma^*$	$E_b/N_0^*$	$\sigma^*$	$E_b/N_0^*$	
4	0.911	0.808	0.904	0.876	0.916	0.757	1.2
5	0.919	0.730	0.911	0.806	0.923	0.691	1.1
6	0.930	0.627	0.907	0.774	0.931	0.622	1.0
7	0.942	0.515	0.922	0.699	0.935	0.577	1.7
8	0.950	0.448	0.938	0.557	0.947	0.468	1.5
9	0.954	0.409	0.940	0.533	0.954	0.411	1.1
10	0.956	0.393	0.942	0.523	0.955	0.403	1.2
11	0.957	0.380	0.942	0.518	0.957	0.377	1.1
12	0.958	0.373	0.942	0.513	0.958	0.367	0.8
15	0.962	0.335	0.944	0.503	0.962	0.340	1.6
20	0.965	0.310	0.946	0.482	0.963	0.325	0.7
30	0.969	0.273	0.946	0.469	0.965	0.299	1.6
50	0.972	0.248	0.952	0.428	0.971	0.260	0.8
RMSE			0.0168	0.1459	0.0031	0.0272	

Table I presents a comparison of thresholds obtained by the proposed method (MC-DE) and those obtained by exact density evolution, for irregular binary<sup>2</sup> LDPC codes with rate 1/2 over the AWGN channel. Thresholds are shown both in terms of noise variance and corresponding  $E_b/N_0$  value. The maximum bit-node degree is reported in the left column; the exact degree distributions  $\lambda$  and  $\rho$  can be found in [1], Tables I and II. For comparison purposes, we have also included threshold values computed by using the Gaussian-Approximation proposed in [14]. At each half-iteration of the Monte-Carlo Density-Evolution (MC-DE) simulation, 10000 outgoing messages are computed, and a maximum number of 500 iterations are executed. For each pair of degree distributions  $(\lambda, \rho)$ , several threshold estimations have been performed; the mean value is reported in the MC-DE/ $\sigma^*$  column, and the standard deviation ( $\times 10^3$ ) is reported in the last column. As it can be observed, the standard deviation is between 0.0008 and 0.0017; hence we conclude that the proposed method is precise. Furthermore, the Root Mean Square Error (RMSE) of estimated thresholds (reported on the last row) is equal to 0.0031, which proves that the proposed method is also accurate.

#### IV. PUNCTURING DISTRIBUTIONS FOR NON-BINARY LDPC CODES

Let a non binary LDPC code be used over a binary-input channel: a non-binary codeword is mapped into its binary images by using (1), then transmitted over the channel. Hence, even if non-binary codes operate at the symbol level, non-binary codewords still can be punctured at the bit-level. A coded symbol can be either completely or partially punctured, according to whether all the bits of its binary image are punctured or not. In order to design good puncturing patterns we have to answer the following questions:

- Assuming that the code is regular, should puncturing bits be clustered or spread over the symbol-nodes? Clustering yields a reduced number of completely punctured symbols, which receive no information from the channel. On the

<sup>2</sup>Exact DE for non-binary LDPC codes over the AWGN channel is not known.

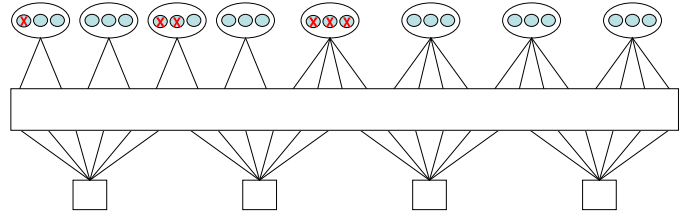


Fig. 2. Bit level puncturing pattern for non-binary LDPC codes

contrary, spreading results into an increased number of partially punctured symbols, which still benefit from some partial information from the channel.

- In case of irregular codes, how should punctured bits be chosen with respect to symbol-node degrees?

Let  $f_{d,k}$  denote the fraction of degree- $d$  symbol-nodes with  $k$  punctured bits. Note that  $\sum_{k=0}^p f_{d,k} = 1$ , as any symbol-node contains either  $k = 0$  (unpunctured), or  $k = 1, \dots$ , or  $k = p$  punctured bits. The overall fraction of punctured bits,  $f$ , and the corresponding punctured rate,  $r_p$ , are given by:

$$f = \frac{1}{p} \sum_{d=1}^{d_s} \sum_{k=0}^p k f_{d,k} L_d, \quad r_p = \frac{r}{1-f}$$

where  $d_s$  is the maximum symbol-node degree, and  $L_d = \frac{\lambda_d}{d \int_0^1 \lambda(x) dx}$  is the fraction of symbol-nodes of degree  $d$ . This is illustrated at Figure 2 for an LDPC code over  $\mathbb{F}_8$  with designed code rate  $r = 1/2$ , where  $f_{2,1} = f_{2,2} = 1/4$ , and  $f_{4,3} = 1/4$ . Thus  $f = 0.25$  and the designed punctured rate is  $r_p = 2/3$ .

#### V. ANALYSIS OF PUNCTURING DISTRIBUTIONS

In this section we analyze different puncturing distributions for regular and semi-regular<sup>3</sup> non-binary LDPC codes over the BIAWGN channel.

First of all, we consider three ensembles of regular LDPC codes with rate 1/2, and (symbol, constraint)-node degrees equal to (2, 4), (3, 6), or (4, 8). A fraction  $f \in [0, 0.25]$  of coded bits are punctured, which corresponds to a punctured rate varying from  $r_p = 1/2$  (no puncturing) to  $r_p = 2/3$ . For each fraction of punctured bits, two puncturing distributions have been compared:

- clustering distribution: punctured bits are clustered on a fraction  $f$  of completely punctured symbols-nodes;
- spreading distribution: if  $f < \frac{1}{p}$  punctured bits are spread over a fraction  $pf$  of symbol-nodes, each one with one single punctured bit. Otherwise, all the symbol-nodes are punctured, each symbol-node containing either  $\lfloor pf \rfloor$  or  $\lceil pf \rceil$  punctured bits

Corresponding thresholds for codes over  $\mathbb{F}_8$  and  $\mathbb{F}_{16}$  are shown respectively at Figure 3 and Figure 4. We note the different behavior of these distributions, depending on the symbol-node degree: the spreading distribution provides better performance for the regular (2, 4) code, but it is outperformed by the clustering distribution for the other two codes with higher symbol-node degrees.

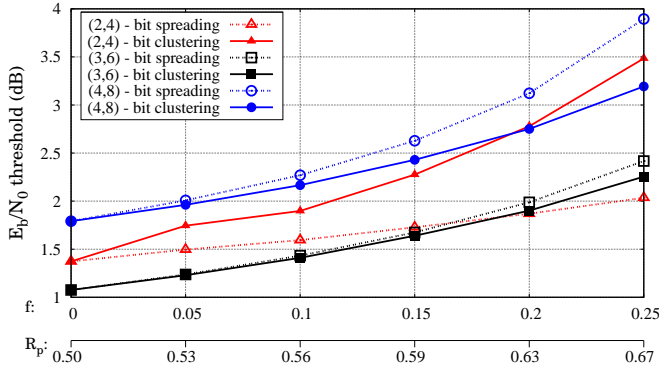


Fig. 3. Spreading vs. clustering distribution; regular LDPC codes over  $\mathbb{F}_8$

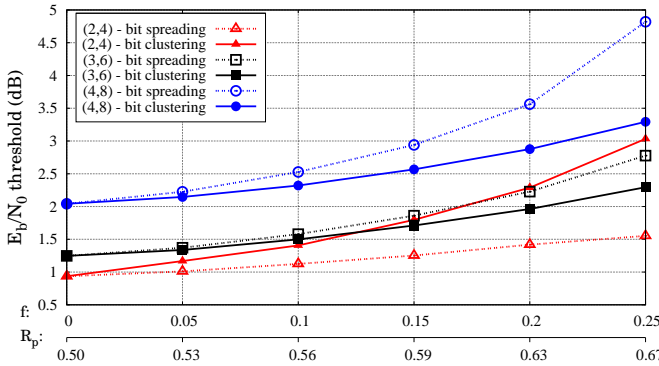


Fig. 4. Spreading vs. clustering distribution; regular LDPC codes over  $\mathbb{F}_{16}$

The intuition behind that goes as follows. An outgoing message from a degree-2 symbol-node depends on the information coming from the channel and the unique incoming extrinsic message. Thus, if a degree-2 symbol-node is completely punctured, it has no channel information, and the outgoing message is equal to the incoming one. This causes a lack of diversity in the iterative message-passing, which results in degraded decoding performance.

Intermediary puncturing distributions can be obtained by mixing the above clustering and spreading distributions, as illustrated at Figure 5 for regular codes over  $\mathbb{F}_4$ : the fraction of punctured bits is  $f = 0.25$ , corresponding to a punctured rate  $r_p = 2/3$ , and it is decomposed as  $f = f_1 + f_2$ , where  $f_1$  is the fraction of bits that are punctured in a spreading manner (in this case, 1 bit per symbol), and  $f_2$  is the fraction of bits that are punctured in a clustering manner (2 bits per symbol). Again, we can observe that the spreading distribution provides better performance for the regular (2,4) code. Similar results are also shown at figure 8 for codes over  $\mathbb{F}_{16}$ : for a clusterization degree  $k \in \{1, 2, 3, 4\}$  (on the abscissa), a fraction  $\frac{1}{k}$  of symbol-nodes are punctured, by punching  $k$  bits per symbol. Once more, we can observe that spreading is suitable for symbol-nodes of degree-2, while clustering is more appropriate for symbol-nodes of degree  $\geq 3$ .

We investigate now different puncturing distributions for semi-regular LDPC codes, with node-perspective degree distribution polynomials  $L(x) = \frac{1}{2}x^2 + \frac{1}{2}x^4$  and  $R(x) = x^6$ ,

<sup>3</sup>With symbol-node degrees taking on two, relatively low, values.

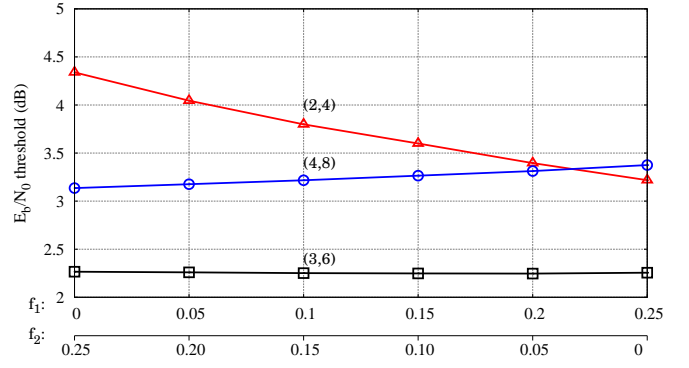


Fig. 5. Intermediary puncturing distributions for regular codes over  $\mathbb{F}_4$

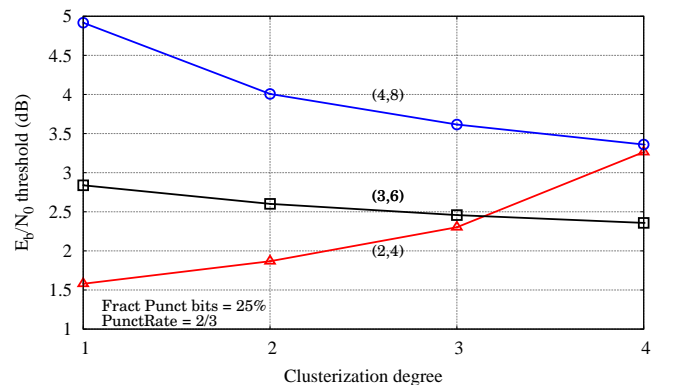


Fig. 6. Various clusterization degrees for regular codes over  $\mathbb{F}_{16}$  for

corresponding to a designed coding rate  $r = 1/2$ . The same fraction  $f = 0.25$  of coded bits are punctured, so as to obtain a punctured rate  $r_p = 2/3$ . The fraction is decomposed as  $f = f_2 + f_4$ , where  $f_2$  is the fraction of bits that are punctured on degree-2 symbol-nodes, and  $f_4$  is the fraction of bits that are punctured on degree-4 symbol-nodes.

Numerical results are shown at Figure 7 and Figure 8: for solid curves, punctured bits are either clustered (full squares) or spread over the symbol-nodes (empty squares), for both symbol-nodes of degree 2 and 4. For the dashed curve, punctured bits are spread over symbol-nodes of degree 2, and clustered over symbol-nodes of degree 4. In view of previous results for regular codes, we were expecting this last distribution to provide the best performance. Surprisingly, it performs in between the clustering and the spreading distribution. What we observe is that in case there are punctured symbols of degree 4 ( $f_4 > 0$ ), the best performance is given by the clustering distribution. However, since all plots correspond to the same punctured rate, the best puncturing distribution in each figure is given by the lowest plot. In both cases this is the distribution that spreads all the punctured bits over symbol-nodes of degree 2 ( $f_2 = 0.25$ ,  $f_4 = 0$ , empty square)<sup>4</sup>. This represents an important dissimilarity compared to the binary case, in which choosing all the punctured bits on degree-2 bit-nodes proves to be catastrophic. In the non-binary case, spreading punctured bits over degree-2 symbol nodes yields

<sup>4</sup>However, the clustering distribution with  $f_2 = 0.2$  and  $f_4 = 0.05$  yields almost the same performance

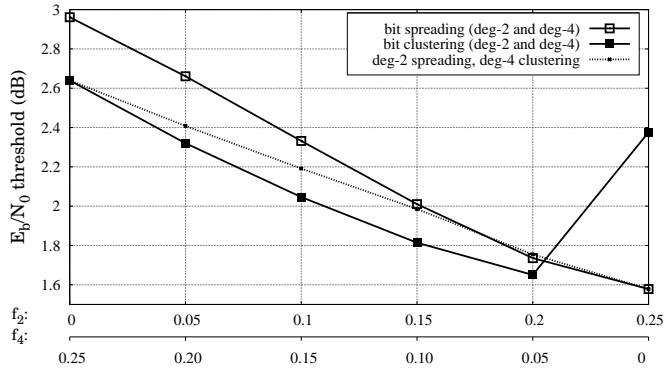


Fig. 7. Low vs. high symbol-degree, and spreading vs. clustering puncturing distributions for irregular LDPC codes over  $\mathbb{F}_8$

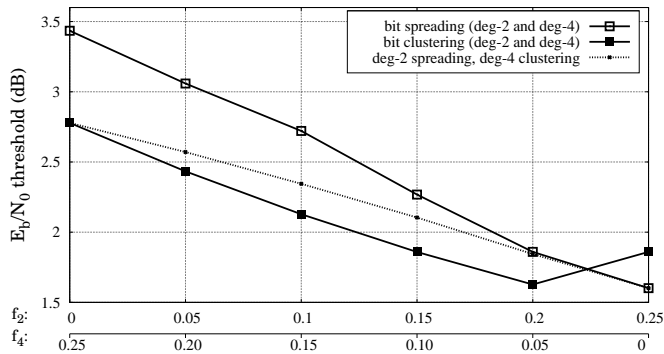


Fig. 8. Low vs. high symbol-degree, and spreading vs. clustering puncturing distributions for irregular LDPC codes over  $\mathbb{F}_{16}$

good performance, provided that the fraction of punctured bits is not too high. The next section will also provide evidence on this fact.

## VI. OPTIMIZATION OF PUNCTURING DISTRIBUTIONS

In this section we present optimized puncturing distributions for an irregular code over  $\mathbb{F}_{16}$  with rate 1/2, and punctured code rates from 0.55 to 0.9. Optimization has been performed by using the Differential Evolution algorithm [15]. First of all we searched for good degree distribution pairs  $\lambda$  and  $\rho$  of rate 1/2, with maximum symbol degree<sup>5</sup> equal to 10. The optimized distributions and the corresponding  $E_b/N_0$  threshold are given below:

$$\begin{aligned} \lambda(x) &= 0.5376x + 0.1678x^2 + 0.1360x^4 + 0.1586x^9 \\ \rho(x) &= 0.5169x^4 + 0.4831x^5 \\ E_b/N_0^* &= 0.3638 \end{aligned}$$

Next, we searched for good puncturing distributions for punctured rates  $r_p \in \{0.55, 0.60, 0.65, 0.70, 0.75, 0.80, 0.85, 0.90\}$ . Optimized distributions  $\{f_{d,k}\}_{d=2,3,5,10, k=0,1,2,3,4}$  for punctured rates 0.60, 0.75, and 0.90 are shown in Table II. Also indicated are  $\bar{k}_d$ , the average number of punctured bits per symbol-node of degree  $d$ , and  $f_k$ , the average fraction of symbols with  $k$  punctured bits. As an equivalent representation, the corresponding clusterization distributions are shown at Figure 9:

<sup>5</sup>Cf. discussion from the Introduction.

TABLE II  
OPTIMIZED DISTRIBUTION,  $r_p = 0.60, 0.75, 0.90$

$r_p = 0.60$	$k = 0$	$k = 1$	$k = 2$	$k = 3$	$k = 4$	$\bar{k}_d$
$d = 2$	0.7132	0.1211	0.1149	0.0083	0.0425	0.5456
$d = 3$	0.5953	0.1536	0.0161	0.0743	0.1607	1.0514
$d = 5$	0.7414	0.0009	0.1822	0.0479	0.0275	0.6190
$d = 10$	0.4608	0.1218	0.1187	0.1109	0.1878	1.4429
$f_k$	0.6865	0.1172	0.1050	0.0257	0.0656	
$r_p = 0.75$	$k = 0$	$k = 1$	$k = 2$	$k = 3$	$k = 4$	$\bar{k}_d$
$d = 2$	0.2026	0.3865	0.1047	0.2757	0.0308	1.5448
$d = 3$	0.3616	0.3680	0.0876	0.1129	0.0699	1.1615
$d = 5$	0.5783	0.0038	0.0435	0.3546	0.0197	1.2335
$d = 10$	0.1998	0.0060	0.3841	0.0230	0.3870	2.3913
$f_k$	0.2545	0.3390	0.1096	0.24585	0.0510	
$r_p = 0.90$	$k = 0$	$k = 1$	$k = 2$	$k = 3$	$k = 4$	$\bar{k}_d$
$d = 2$	0.0960	0.4187	0.1077	0.2857	0.0919	1.8589
$d = 3$	0.6543	0.0070	0.0779	0.1035	0.1572	1.1023
$d = 5$	0.1304	0.3957	0.1314	0.2905	0.0521	1.7384
$d = 10$	0.0413	0.0132	0.2822	0.3780	0.2854	2.8530
$f_k$	0.1811	0.3369	0.1125	0.2623	0.1072	

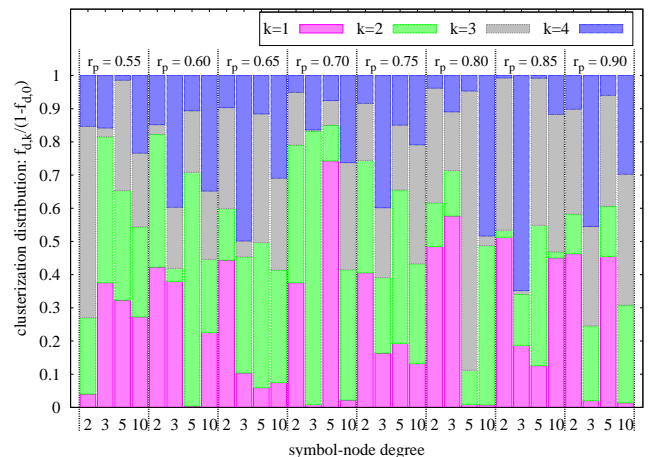


Fig. 9. Clusterization distributions for  $r_p \in \{0.55, \dots, 0.90\}$

they consist of fractions of punctured symbols<sup>6</sup> of degree- $d$ , with  $k$  punctured bits per symbol, which are given by  $\frac{f_{d,k}}{1-f_{d,0}}$ , for  $d = 2, 3, 5, 10$ , and  $k = 1, \dots, 4$ . These distributions seem to be random, and properties observed for regular codes shall not apply in this case.

Thresholds of optimized punctured distributions are shown at Figure 10, in terms of  $E_b/N_0$ . Are also plotted the theoretical Shannon limit (capacity), and thresholds of distributions spreading punctured bits over degree-2 symbol-nodes. The gap between optimized distributions and capacity vary between 0.18 dB for  $r_p = 0.5$  (unpunctured code) and 0.52 dB for  $r_p = 0.9$ . We also note that the degree-2-spreading distribution yields very good performance up to punctured rate  $r_p = 0.7$ . However, such a puncturing distribution proves to be catastrophic for punctured rates  $r_p \geq 0.85$

Finally, Figure 11 presents the Frame Error Rate performance of optimized distributions for finite code lengths. All the codes have binary dimension (number of source bits)

<sup>6</sup>Recall that  $f_{d,k}$  is the fraction of symbols of degree- $d$ , with  $k$  punctured bits per symbol

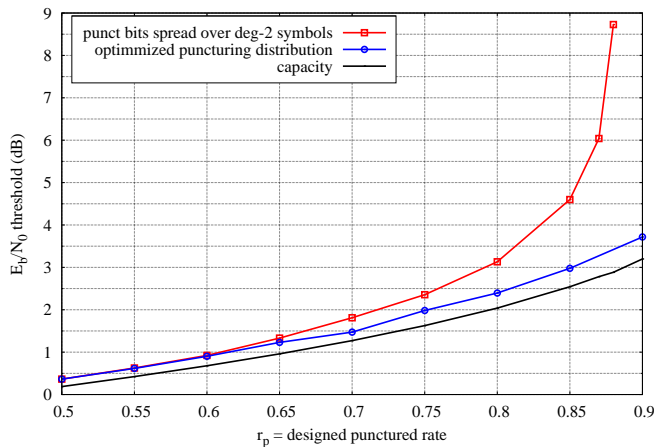


Fig. 10. Optimized puncturing distributions for regular codes over  $\mathbb{F}_{16}$

equal to 4000 bits (1000  $\mathbb{F}_{16}$ -symbols). The mother code with rate 1/2 has been constructed by using the Progressive Edge Growth (PEG) algorithm [16], and punctured patterns have been randomly chosen according to the optimized distribution. It is very likely that the performance can be further improved by using an optimized design of the puncturing patterns (in terms of symbol-recoverability steps, cf. discussion in the introduction), especially for high punctured rates.

## VII. CONCLUSIONS

Except for simple channel models, as for instance the binary erasure channel, it is generally an arduous task to derive exact density evolution for non-binary LDPC codes. Yet, even if the exact density evolution were known, its inherent complexity would certainly prohibit its use for optimization purposes.

In this paper we proposed a density evolution approximation method, by using Monte-Carlo simulation of an infinite code. The proposed method provides accurate and precise estimates of non-binary ensemble thresholds, and makes possible the optimization of non-binary codes for a wide range of applications and channel models.

As an application, rate-adaptability solutions for non-binary LDPC codes have been investigated. Puncturing distributions for regular and irregular codes have been analyzed by using simulated density evolution thresholds of non-binary LDPC codes over the AWGN channel. For regular codes, we showed that the design of puncturing patterns must respect different rules depending on the symbol-node degree: punctured bits must be spread over degree-2 symbol-nodes, while they must be clustered on symbol-nodes of higher degrees. If the number of punctured bits is relatively small, spreading punctured bits over degree-2 symbol-nodes yields also good performance for irregular codes. However, such a puncturing distribution could be catastrophic for higher punctured rates, in which case optimized puncturing distributions are indispensable. Finally, we presented optimized puncturing distributions for non-binary LDPC codes with small maximum degree, which exhibit a gap to capacity between 0.2 and 0.5 dB, for punctured rates varying from 0.5 to 0.9.

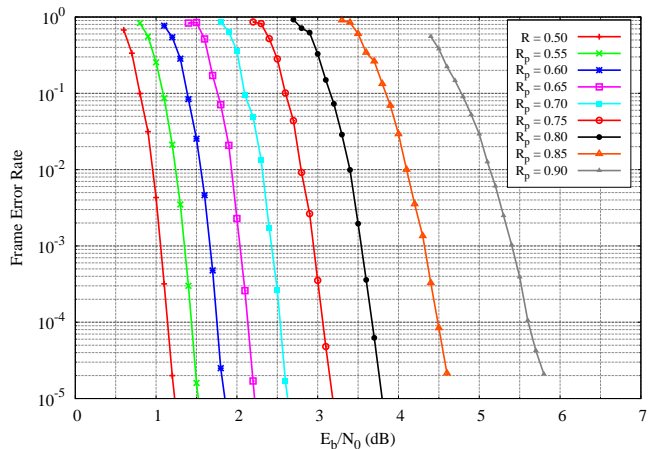


Fig. 11. Frame error rate, optimized distributions,  $K = 4000$  bits

## REFERENCES

- [1] T. J. Richardson, M. A. Shokrollahi, and R. L. Urbanke, "Design of capacity approaching irregular low density parity check codes," *IEEE Trans. Inform. Theory*, vol. 47, no. 2, pp. 619–637, 2001.
- [2] M. C. Davey and D. J. C. MacKay, "Low density parity check codes over GF(q)," *IEEE Commun. Lett.*, vol. 2, pp. 165–167, 1998.
- [3] D. Declercq and M. Fossorier, "Decoding algorithms for non-binary LDPC codes over GF(q)," *IEEE Trans. Commun.*, vol. 55, no. 4, pp. 633–643, 2007.
- [4] V. Savin, "Min-Max decoding for non binary LDPC codes," in *IEEE Int. Symp. on Information Theory*, July 2008.
- [5] J. Ha, J. Kim, and S. W. McLaughlin, "Rate-compatible puncturing of low-density parity-check codes," *IEEE Transactions on information Theory*, vol. 11, November 2004.
- [6] D. Klinc, J. Ha, and S.W McLaughlin, "On rate-adaptability of non-binary LDPC codes," in *5th International Symposium on Turbo codes and related topics*, 2008.
- [7] J. Ha, J. Kim, D. Klinc, and S.W. McLaughlin, "Rate compatible punctured low-density parity-check codes with short block lengths," *IEEE Trans. on Inform. Theory*, vol. IT-52, pp. 728–738, 2006.
- [8] T. J. Richardson and R. L. Urbanke, "The capacity of low-density parity-check codes under message-passing decoding," *IEEE Trans. Inform. Theory*, vol. 47, no. 2, pp. 599–618, 2001.
- [9] V. Rathi and R. Urbanke, "Thresholds and the stability condition for non-binary LDPC codes," *IEE Proceedings Communication*, vol. 152, no. 6, 2005.
- [10] V. Savin, "Non binary LDPC codes over the binary erasure channel: density evolution analysis," in *IEEE Int. Symp. Applied Sciences on Biomedical and Communication Technologies (ISABEL)*, 2008.
- [11] G. Li, I. J. Fair, and W. A. Krzymie, "Density evolution for nonbinary LDPC codes under gaussian approximation," *IEEE Trans. Inform. Theory*, vol. 55, no. 3, March 2009.
- [12] M. C. Davey and D. J.C. MacKay, "Monte Carlo simulations of infinite low density parity check codes over GF(q)," in *International Workshop on Optimal Codes and Related Topics (OC98)*, 1998.
- [13] N. Wiberg, *Codes and decoding on general graphs*, Ph.D. thesis, Lkoping University, 1996, Sweden.
- [14] S.-Y. Chung, T.J. Richardson, and R.L. Urbanke, "Analysis of sum-product decoding of low-density parity-check codes using a Gaussian approximation," *IEEE Trans. Inform. Theory*, vol. 47, no. 2, pp. 657–670, 2001.
- [15] R. Storn and K. Price, "Differential evolution - a simple and efficient heuristic for global optimization over continuous spaces," *Journal of Global Optimization*, vol. 11, pp. 341–359, 1997.
- [16] X. Y. Hu, E. Eleftheriou, and D. M. Arnold, "Regular and irregular progressive edge-growth tanner graphs," *IEEE Trans. Inform. Theory*, vol. 51, no. 1, pp. 386–398, 2005.